

This is a repository copy of *Experimental Methods for Evaluating the Bacterial Uptake of Trojan Horse Antibacterials*.

White Rose Research Online URL for this paper:

<https://eprints.whiterose.ac.uk/id/eprint/169022/>

Version: Accepted Version

---

**Article:**

Southwell, James W, Black, Conor M and Duhme-Klair, Anne-Kathrin orcid.org/0000-0001-6214-2459 (2020) Experimental Methods for Evaluating the Bacterial Uptake of Trojan Horse Antibacterials. ChemMedChem. ISSN 1860-7179

<https://doi.org/10.1002/cmdc.202000806>

---

**Reuse**

Items deposited in White Rose Research Online are protected by copyright, with all rights reserved unless indicated otherwise. They may be downloaded and/or printed for private study, or other acts as permitted by national copyright laws. The publisher or other rights holders may allow further reproduction and re-use of the full text version. This is indicated by the licence information on the White Rose Research Online record for the item.

**Takedown**

If you consider content in White Rose Research Online to be in breach of UK law, please notify us by emailing [eprints@whiterose.ac.uk](mailto:eprints@whiterose.ac.uk) including the URL of the record and the reason for the withdrawal request.

# Experimental Methods for Evaluating the Bacterial Uptake of Trojan Horse Antibacterials

James W. Southwell<sup>+[a]</sup>, Conor M. Black<sup>+[a]</sup> and Anne-Kathrin Duhme-Klair<sup>+[a]</sup>

[a] Mr. J. W. Southwell, Mr. C. M. Black, Prof. A.-K. Duhme-Klair  
Department of Chemistry  
University of York  
Heslington, North Yorkshire, YO10 5DD (United Kingdom)  
E-mail: anne.duhme-klair@york.ac.uk

**Abstract:** The field of antibacterial siderophore conjugates, referred to as Trojan Horse antibacterials, has received increasing attention in recent years, driven by the rise of antimicrobial resistance. Trojan Horse antibacterials offer an opportunity to exploit the specific pathways present in bacteria for active iron uptake, potentially allowing the bypassing of membrane-associated resistance mechanisms. Hence, the Trojan Horse approach may enable the redesigning of old antibiotics and the development of antibacterials that target specific pathogens. A critical part of evaluating such Trojan Horse antibacterials and improving their design is the quantification of their bacterial uptake, and the identification of the pathways by which this occurs. In this minireview, we highlight a selection of the biological and chemical methods used to study the uptake of Trojan Horse antibacterials, exemplified with case studies, some of which have led to drug candidates in clinical development or approved antibiotics.

## 1. Introduction

### 1.1 Siderophores

Iron is an essential resource to almost all living organisms, however its availability can be limited due to the poor aqueous solubility of its dominant oxidation state,  $\text{Fe}^{3+}$  (ferric iron). To overcome this limitation, organisms have developed regulatory systems for iron uptake, storage and distribution. Siderophores are low-molecular weight compounds produced by bacteria (and fungi) that are released into their surrounding medium to selectively bind to  $\text{Fe}^{3+}$  and facilitate its uptake. To satisfy the coordination requirements of  $\text{Fe}^{3+}$  and enable its preferred octahedral coordination geometry, siderophores are typically composed of three bidentate chelator motifs dominated by hard, negatively charged oxygen atoms (Figure 1). To date, more than 250 siderophores have been discovered and characterised,<sup>[1]</sup> examples of which include enterobactin, desferrioxamine and pyoverdine PVD1 (Figure 2).

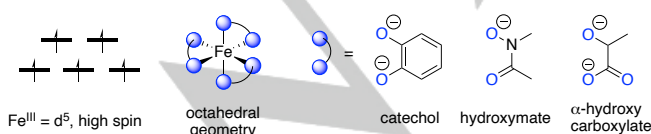


**Figure 1.** Electronic configuration and preferred coordination geometry of  $\text{Fe}^{3+}$ , and examples of bidentate chelators used in siderophores.

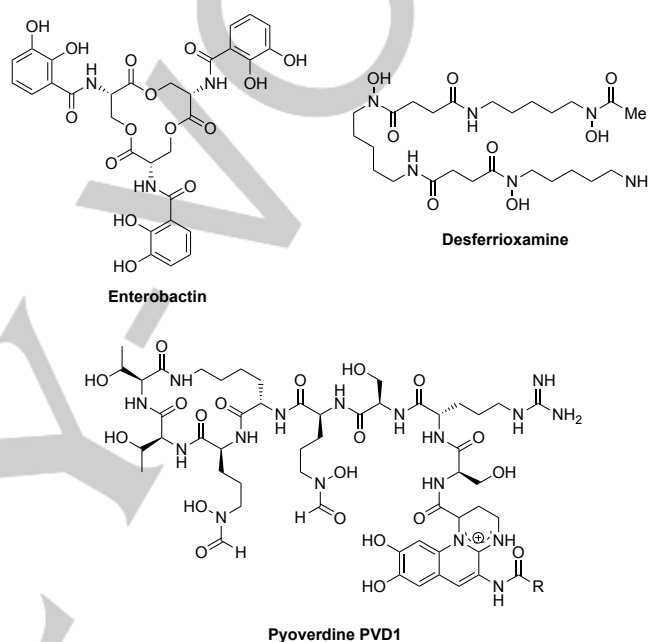


**Figure 2.** Structures of enterobactin, desferrioxamine and pyoverdine (PVD1, *Pseudomonas aeruginosa*).

### 1.2 Siderophore-mediated Iron Transport in Bacteria

After siderophores are released into the extracellular environment and have acquired  $\text{Fe}^{3+}$ , the resulting complexes are recognised and bound by specific cell-surface receptors, for example FepA in *Escherichia coli* (*E. coli*), which is specific for enterobactin.<sup>[2]</sup> In Gram-negative bacteria, the  $\text{Fe}^{3+}$ -siderophore complex is then actively transported through the outer membrane *via* interaction of the receptors with a TonB complex on the inner membrane.<sup>[1]</sup> Inside the periplasm, the complexes bind to cognate periplasmic binding proteins (e.g. FepB for enterobactin in *E. coli*), and are then shuttled to ABC transporters for transfer to the cytoplasm through the inner membrane. As Gram-positive species do not possess two membranes, specific cell-surface receptors transfer the iron-siderophore complexes directly through similar ABC transporters into the cytoplasm.<sup>[1]</sup> Iron is released from the siderophore *via* reducing and/or hydrolysing enzymes (e.g. Fes for enterobactin in *E. coli*).<sup>[3]</sup> A schematic summarising these uptake mechanisms is shown in Figure 3.

## MINIREVIEW

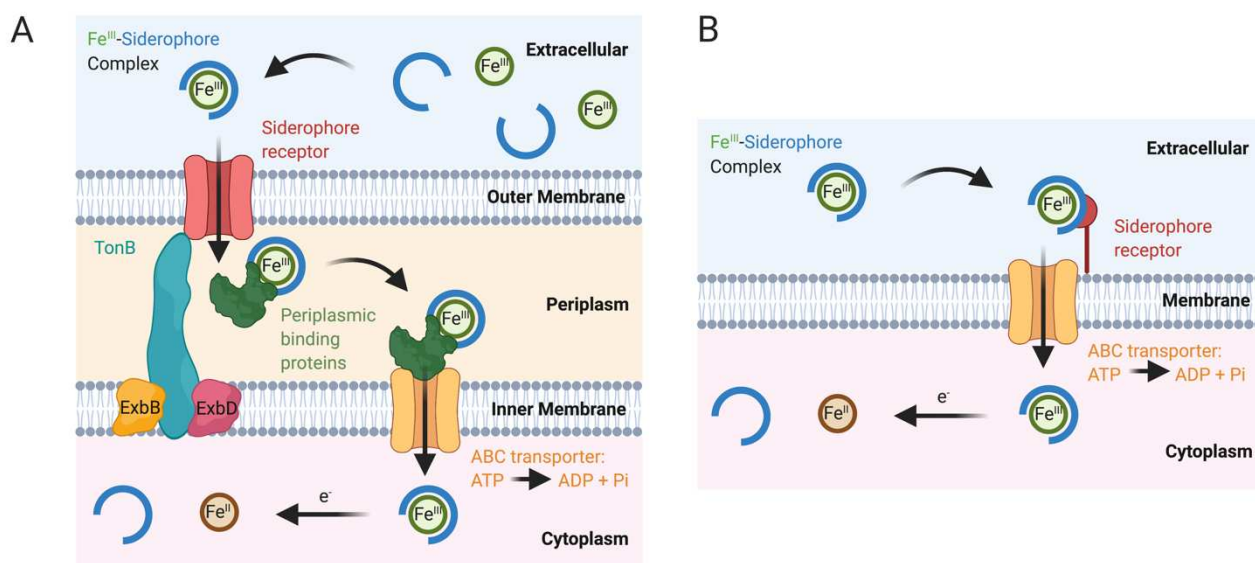


**Figure 3.** Schematic of siderophore-mediated iron uptake into (A) a Gram-negative and (B) a Gram-positive bacterial cell. Figure created with BioRender.com.

### 1.3 Regulation of Iron Uptake

Iron uptake pathways in bacteria are upregulated in response to iron-limiting conditions, for example those imposed by host organisms.<sup>[1]</sup> In Gram-negative bacteria, the biosynthesis of siderophores and expression of cell-surface receptors is primarily regulated by the  $\text{Fe}^{2+}$ -dependent repressor protein Fur. On binding intracellular  $\text{Fe}^{2+}$ , Fur binds in turn to regulatory DNA sequences, repressing the transcription of the genes involved in iron uptake.<sup>[4,5]</sup> Therefore, low intracellular  $\text{Fe}^{2+}$  levels result in upregulation of these genes. Similar repressor proteins are known to exist in Gram-positive bacteria.<sup>[1]</sup>

### 1.4 Trojan Horse Antibacterials

In order to better compete for survival, some bacteria have developed antibacterial-siderophore conjugates, termed sideromycins. One such example is albomycin, produced by *Streptomyces* sp. (Figure 4).<sup>[6]</sup> Disguised as useful siderophores, these conjugates are taken up into bacteria where the antibacterial component then causes cell death. Due to analogies made with the wooden horse used to conquer the city of Troy in Greek mythology, these conjugates are often referred to as Trojan Horse antibacterials (THAs). This strategy has inspired numerous investigations from both academia and industry into the design of novel antibiotics. In recent years, THAs have met with some success, with a number of drug candidates entering clinical trials and cefiderocol (Fetroja) subsequently being approved by the U.S. Food and Drug Administration (FDA) for the treatment of complicated urinary tract infections (cUTIs) (Figure 4).<sup>[7–9]</sup>

### 1.5 The Importance of Studying Bacterial Uptake Mechanisms

The overall efficacy of antibacterials is influenced by a combination of properties such as drug-target binding, efflux, drug alteration/degradation and bacterial uptake. Understanding the relative contributions of each of these parameters on antibacterial potency is vital for drug evaluation and optimisation. Thus, an important part in the investigation of THAs is the quantification of their bacterial uptake and identification of the mechanisms that

James Southwell is a final-year PhD student in the groups of Prof. Anne-Kathrin Duhme-Klair and Prof. Keith Wilson at the University of York, having graduated with an MChem from the University of York in 2017, with a year in industry at Redx Pharma. His research includes the development of siderophore-conjugated bioorthogonal catalysts for the activation of antibiotics inside bacteria.



Conor Black is a final-year PhD student in the groups of Prof. Anne-Kathrin Duhme-Klair and Dr. Anne Routledge at the University of York, having graduated with an MChem from the University of Warwick in 2017. His research includes the development of new biolabile linkers for siderophore-based Trojan Horse conjugates.



Anne-Kathrin Duhme-Klair is a Professor of Biological Inorganic Chemistry in the Department of Chemistry at the University of York, with research interests in the areas of bioinorganic and medicinal inorganic chemistry. She obtained her PhD in Inorganic Chemistry at the University of Oldenburg. After postdoctoral positions at King's College London and the EMBL Outstation at DESY in Hamburg, she completed her Habilitation at the University of Münster. The focus of her current research includes siderophore-mediated iron uptake, artificial metalloenzymes and the development of Trojan Horse antimicrobials.



## MINIREVIEW

facilitate this uptake. In circumstances where the redesign of existing antibiotics by the attachment of siderophores aims to bypass access-related resistance, confirmation of their uptake via the targeted iron transport pathways is especially important.

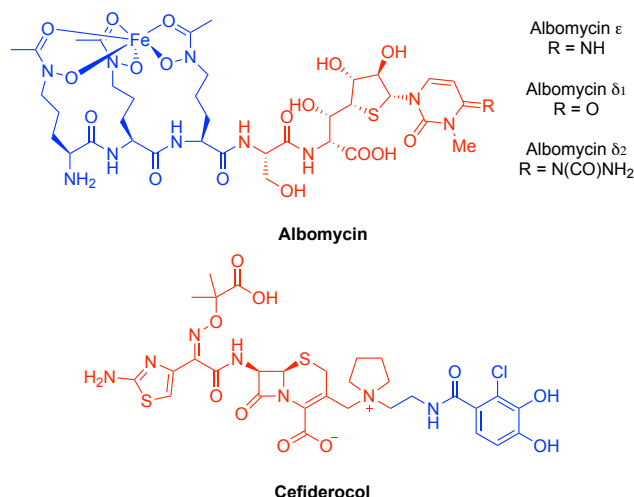


**Figure 4.** Structure of albomycin and cefiderocol (Fetroja). Antibacterial parts in red and siderophore parts in blue.

Herein, we summarise the various experimental methods that have been employed to determine and quantify the uptake of THAs into bacterial cells (Figure 5) and in some cases identify the mechanisms that facilitate this uptake. This minireview is in no way exhaustive, as we aim to briefly summarise the various methods alongside a few select case studies. Although Trojan Horse strategies are not limited to the delivery of antibacterials, this review focuses on their applications in this area.

## 2. Iron-dependent Antibacterial Activity

The determination of minimum inhibitory concentrations (MICs) is an important part of any antibacterial investigation. In order to gain accurate and informative antibacterial profiles, the growth media utilised in such studies should ideally reflect those imposed by the targeted host organism. For pathogenic bacteria living inside a human host, their access to iron is limited due to competition with the human iron-sequestering protein transferrin and the native microbiome. In blood serum, for example, iron concentrations are reported as  $\approx 10^{-24}$  M.<sup>[10]</sup> Therefore, bacterial growth media utilised for investigating THAs are often iron-depleted. A commonly used medium for MIC determination is Mueller-Hinton Broth II (MHII). To lower levels of concomitant iron, MHII is often pre-treated with an iron-binding Chelex® resin and made up using acid-treated glassware. Notably, the activity of FDA-approved THA cefiderocol was determined using these conditions.<sup>[11]</sup> In some cases, synthetic chelators such as 2, 2'-bipyridine (bpy) (Figure 6), are added to bind to and withhold iron, thereby enforcing greater iron-limitation. Whilst the use of bpy is most common for the determination of MICs under iron-limited conditions, alternative chelators such as divin (Figure 6) or human transferrin have also been utilised to enforce iron-limitation.<sup>[12,13]</sup>

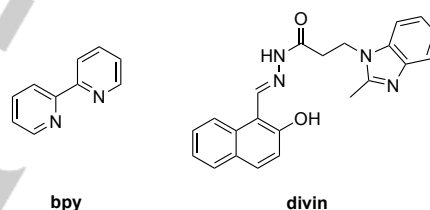


**Figure 6.** Structures of 2,2'-bipyridine (bpy) and divin.

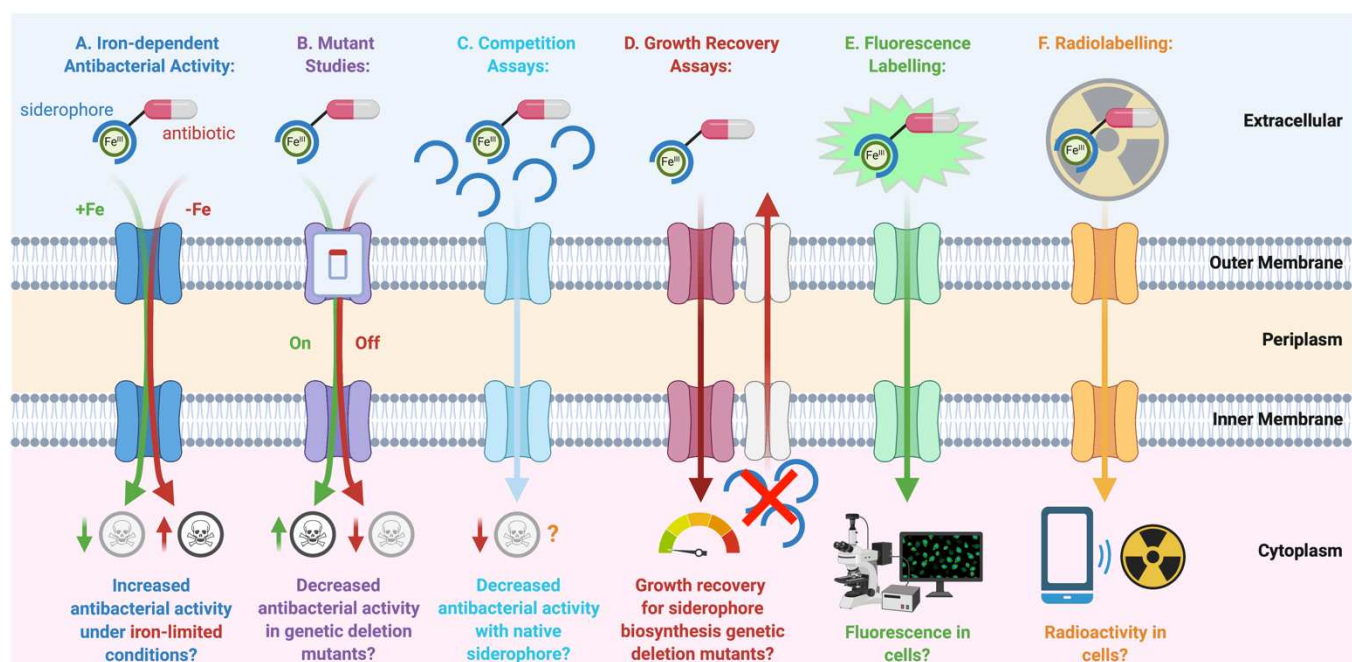


**Figure 5.** Summary for experimental methods utilised to evaluate the bacterial uptake of Trojan Horse antibacterials: (A) iron-dependent antibacterial activity, (B) mutant studies, (C) competition assays, (D) growth recovery assays, (E) fluorescence labelling, (F) radiolabelling. Figure created with BioRender.com.

## MINIREVIEW

It is common for the MICs of THAs to be determined against bacteria grown in both iron-limited and iron-sufficient conditions (Figure 5A). As iron uptake pathways are upregulated in response to iron-limitation, an inverse correlation between iron concentration and antibacterial activity is often used to infer the utilisation of siderophore transport pathways by THA candidates.<sup>[11,14–21]</sup> A recent example can be found in work by Goldberg *et al.* in the development of a  $\gamma$ -lactam-monocatechol conjugate, YU253434 (Figure 7).<sup>[18]</sup> After observing encouraging potencies against *Pseudomonas aeruginosa* (*P. aeruginosa*) PAO1, the MIC of YU253434 was re-determined in iron-limited MHII at various concentrations of supplemented iron(III) chloride. Encouragingly, the MIC increased with iron concentration in a similar fashion to the known THA cefiderocol, suggesting siderophore-mediated uptake into the periplasm (Table 1), whereas no MIC change was observed for control compound ceftazidime (Figure 7). Iron-dependent antibacterial activity studies can also be undertaken using agar plates, and measuring the change in the zone of inhibition, between iron-limited and iron-sufficient conditions.<sup>[22]</sup>

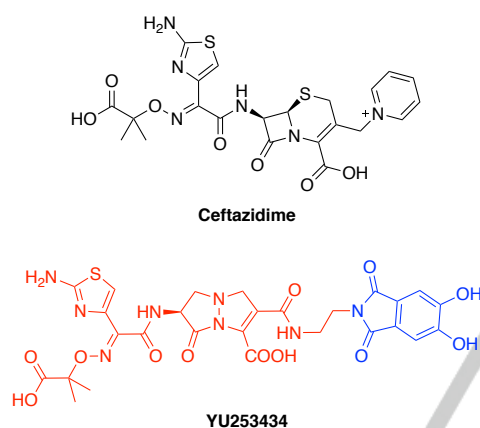


**Figure 7.** Structures of YU253434 and ceftazidime.<sup>[18]</sup> For YU253434, antibacterial part in red and siderophore part in blue.

**Table 1.** MIC data for YU253434, ceftazidime and cefiderocol against *P. aeruginosa* (PAO1), with varied iron concentration.<sup>[18]</sup>

added iron ( $\mu\text{g mL}^{-1}$ )	MIC ( $\mu\text{g mL}^{-1}$ )		
	YU253434	ceftazidime	cefiderocol
0	0.5	1	0.06
0.1	2	1	0.25
1.0	16	1	0.5
10	>16	1	2

Previously, Zheng and Nolan investigated amoxicillin (Amx) and ampicillin (Amp) conjugates of enterobactin, **THA-1** (Ent-Amx) **THA-2** (Ent-Amp), (Figure 8).<sup>[16]</sup> As enterobactin is the main siderophore of *E. coli*, MIC investigations were performed with the common laboratory strain *E. coli* K12. A 50% MHII medium in the presence and absence of 200  $\mu\text{M}$  bpy was used to enforce iron-limited and iron-sufficient conditions, respectively. Results showed a 100-fold decrease in MIC for synthesised THAs tested against bacteria grown under iron-limitation, where Amx and Amp

controls showed negligible change (Figure 9). In addition, when native enterobactin was administered in a 1:1 ratio with Amx or Amp, no increased activity was observed compared to each antibiotic individually, indicating siderophore-antibiotic conjugation was required for the improved antibacterial activity. Possible antibacterial activity due to iron sequestration was examined through MIC determination of the iron-bound versions of **THA-1** and **THA-2**. The close similarity of these MIC values compared to that of their iron-free versions indicated negligible iron sequestration.<sup>[16]</sup>

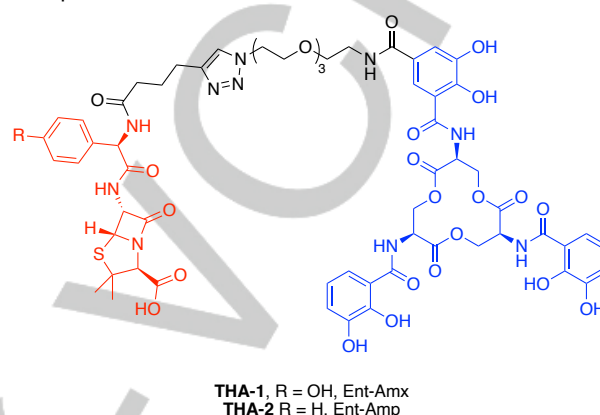


**Figure 8.** Structures of **THA-1** and **THA-2**.<sup>[16]</sup> Antibacterial parts in red and siderophore parts in blue.

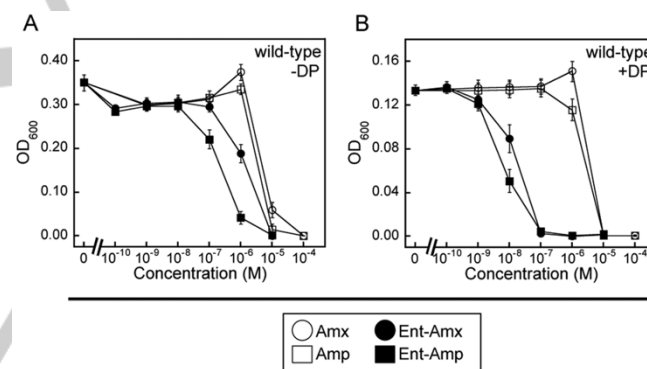


**Figure 9.** Dose dependency of **THA-1**, **THA-2** against *E. coli* K12 under iron-sufficient (A) and bpy (DP)-induced iron-limited (B) conditions versus their corresponding amoxicillin/ampicillin controls.<sup>[16]</sup> Reprinted from T. Zheng and E. M. Nolan, *J. Am. Chem. Soc.*, 2014, 136, 27, 9677-9691, <https://pubs.acs.org/doi/full/10.1021/ja503911p>, with permission from ACS.

## 2.1 Summary

Although iron-dependent antibacterial activity experiments can be informative, it is important to probe the contribution of iron sequestration-associated toxicity using iron-bound THA controls, otherwise any observed antibacterial activity due to iron starvation can be misinterpreted as the desired drug-target inhibition. As a result, such experiments are usually employed alongside complementary studies, such as mutant studies and imaging techniques (see later sections).

## 3. Mutant Studies

As detailed above, there are a number of key cellular components involved in siderophore-mediated iron uptake pathways. A

## MINIREVIEW

common technique in studying THAs, and siderophores in general, is the use of genetic deletion mutants to interrogate these key components. Indeed, for many commonly used species like *E. coli*, large libraries of such mutants already exist. By examining changes in THA sensitivity between wild-type and genetic deletion mutant strains, the involvement of the deleted components in THA transport can be inferred (Figure 5B).

In 1990, Nikaido and Rosenberg investigated the uptake of  $\beta$ -lactam conjugates of catechols and analogues into *E. coli*.<sup>[23]</sup> The MIC values for each of pirazmonam, U-78,608 and E0702 (Figure 10) were determined against a variety of siderophore transport related *E. coli* genetic deletion mutants, where significant increases in MIC were observed against a  $\Delta fiu\Delta cir$  double mutant (Table 2). These results suggested that the conjugates tested use

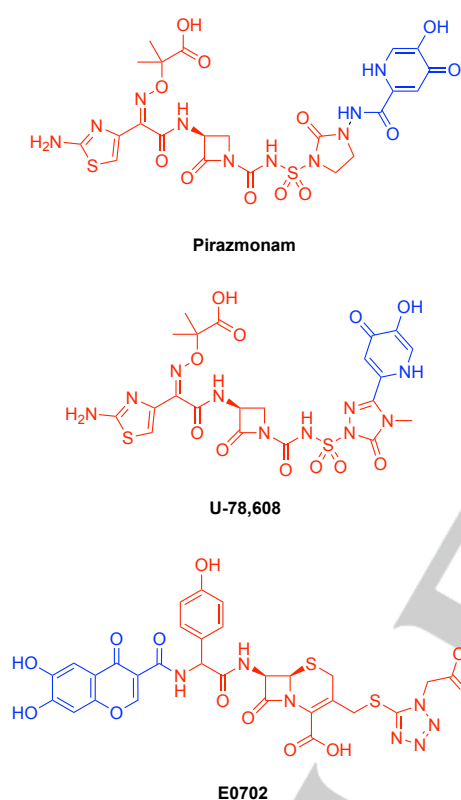


**Figure 10.** Structures of pirazmonam, U-78,608 and E0702.<sup>[23]</sup> Antibacterial parts in red and siderophore parts in blue.

**Table 2.** MIC data for pirazmonam, U-78,608 and E0702 against various wild-type and genetic deletion mutants of *E. coli*.<sup>[23]</sup>

<i>E. coli</i> strain	relevant genotype(s)	MIC ( $\mu\text{g mL}^{-1}$ )		
		pirazmonam	U-78,608	E0702
MC4100	Wild-type	0.1	0.1	0.05
W3100	Wild-type	0.2	0.2	0.1
JK116	$\Delta cir$	2.0	0.6	3.2
HN593	$\Delta cir\Delta fiu$	6.2	3.1	25.6

the corresponding receptor proteins (Fiu and Cir) for penetration of the outer membrane. Fiu and Cir are thought to be outer membrane transporters for complexes of iron with bidentate catecholates, such as the hydrolysis products of enterobactin.<sup>[24]</sup> Significant increases in MIC were also observed for a  $\Delta tonB$  mutant, which is deficient in all siderophore-mediated transport. This supports the use of siderophore transport pathways, and also indicates a lack of uptake via other pathways such as porins.

In 2012, McPherson *et al.* realised the importance of two siderophore receptors in *P. aeruginosa*, PiuA and PirA, for the uptake of  $\beta$ -lactam THAs BAL30072 and MC-1 (Figure 11), by investigating their effects on the growth of corresponding genetic deletion mutants,  $\Delta piuA$  and  $\Delta pirA$ , respectively.<sup>[20]</sup> It was found that the MIC values of these THAs were increased for the  $\Delta piuA$  mutant, indicating that this TonB-dependent receptor and member of the Fiu family, facilitated uptake (Table 3). Although negligible MIC change was observed for the single  $\Delta pirA$  mutant, MIC values did increase significantly for the  $\Delta piuA\Delta pirA$  double mutant, indicating the enterobactin receptor PirA was also involved but likely as a secondary uptake route. In 2017, Moynié *et al.*<sup>[25]</sup> identified two homologous receptors in *Acinetobacter baumannii* also important to BAL30072 and MC-1 activity.<sup>[20,26]</sup>

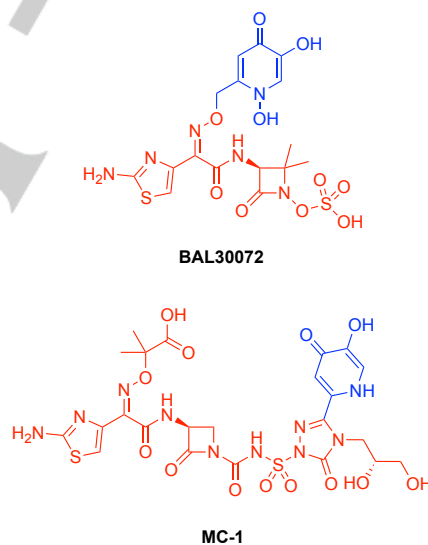


**Figure 11.** Structures of BAL30072 and MC-1.<sup>[20,26]</sup> Antibacterial parts in red and siderophore parts in blue.

**Table 3.** MIC data for MC-1 and BAL30072 against various wild-type and genetic deletion mutants of *P. aeruginosa*.<sup>[20]</sup>

relevant genotype(s)	MIC ( $\mu\text{g mL}^{-1}$ )			
	MC-1		BAL30072	
	+Fe	-Fe	+Fe	-Fe
PAO1	0.25	0.25	4	2
$\Delta piuA$	8	0.25	16	2
$\Delta pirA$	0.5	0.25	4	2
$\Delta piuA\Delta pirA$	32	32	64	64

## MINIREVIEW

Mutations in iron uptake pathways are often implicated in the emergence of spontaneous resistance during antibacterial screening. During screening of MC-1, McPherson *et al.* observed *P. aeruginosa* mutants with decreased expression of the PiuA receptor as a result of a mutation in the adjacent *piuC* gene; similar observations were made by van Delden *et al.* for BAL-30072, alongside upregulation of the FecIRA pathway for citrate transport, which may draw cellular resources away from the expression of the outer membrane receptors required for uptake.

[20,26]

### 3.1 Summary

The use of genetic deletion mutants is not only useful for the identification of outer membrane receptors involved in the uptake of THAs, but also subsequent parts of the uptake pathway. Moreover, the use of mutant strains is not limited to MIC variation studies; genetic deletion mutants can also be used in various different experiment types such as growth recovery and competition assays (see later sections). These experiments are straightforward if the required mutant strains are available, however, in some cases the desired mutants are not available for purchase and must be specifically produced.

## 4. Competition Assays

When bacteria are exposed to a toxic concentration of a THA capable of hijacking siderophore transporters, THA uptake *via* siderophore-mediated pathways is competitive with that of native siderophores. Once levels of native siderophores are sufficiently high, they will outcompete the THA for uptake, thus decreasing its antibacterial activity. Hence, if the activity of a prospective THA is perturbed by the addition of a native siderophore, this is indicative of competition for the same cellular uptake pathway. Such experiments are commonly denoted as competition assays (Figure 5C).

In 2013, Wenciewicz *et al.* utilised competition assays to infer the uptake of the ciprofloxacin-danoxamine conjugate **THA-3**, (Figure 12).<sup>[15]</sup> Although iron-dependent antibacterial assays showed promise against *S. aureus*, it was important to obtain further evidence for siderophore-mediated uptake *via* FhuD. As FhuD is known to be involved in the uptake of hydroxamate-type siderophores, such as desferrioxamine B (DFO) in *S. aureus*, an activity reduction of **THA-3** on co-administration with DFO would be supportive of bacterial uptake *via* this transporter. Indeed, the MIC of **THA-3** was increased >100-fold in the presence of DFO under iron-limited conditions.

The development of carbapenem-siderophore conjugates MC-1 and MB-1 (Figure 13) by Tomaras *et al.*<sup>[27]</sup> included competition assays. It was noticed that *P. aeruginosa* MB-1 resistant colonies grown on iron-limited MHII agar plates were surrounded by a 'fluorescent yellow-green haze' suspected to be pyoverdine, one of the native siderophores produced by *P. aeruginosa*. To confirm this hypothesis, the medium of a wild-type PAO1 culture grown in iron-limited MHII was added at various concentrations to a genetic deletion mutant ( $\Delta pvdA$ ), incapable of pyoverdine biosynthesis, and the MIC values for MB-1 were measured. As anticipated, the MIC increased upon addition of the pyoverdine-containing PAO1

media, suggesting that the presence of pyoverdine in the media hindered THA uptake, either by outcompeting MB-1 for iron binding and/or by driving the downregulation of non-pyoverdine uptake pathways. Additional studies showed that the addition of as little as 200 nM pyoverdine or enterobactin increased the MIC of MB-1 16- and 4-fold respectively.

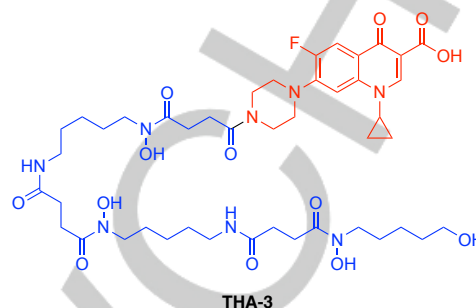


**Figure 12.** Structure of **THA-3**.<sup>[15]</sup> Antibacterial part in red and siderophore part in blue.

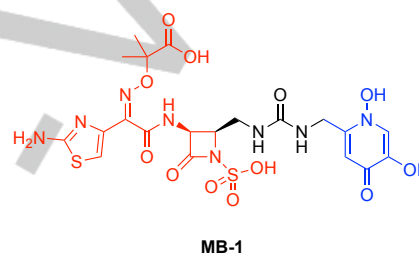


**Figure 13.** Structure of MB-1.<sup>[27]</sup> Antibacterial part in red and siderophore part in blue.

### 4.1 Summary

Competition assays are informative experiments, best employed after MIC determination in iron-limited media. As with iron-dependent antibacterial activity studies, it is important to consider the iron sequestration-associated antibacterial activity of THAs when carrying out competition assays. Even if the antibacterial activity of a THA decreases upon addition of a native siderophore, this effect may be due to the negating of iron-starvation associated THA toxicity rather than competition for the same siderophore receptor. Therefore, competition assays are best employed in parallel with supporting studies.

## 5. Growth Recovery Assays

If siderophore utilisation in bacteria is impeded to the extent of iron-deficiency, bacterial growth is diminished. In cases where the insufficient iron supply is a result of genetic deletion related to siderophore biosynthesis, growth recovery observed on addition of a prospective THA can be used to infer their mimicking of siderophores (Figure 5D). If there is then reduced growth recovery for genetic deletion mutants related to siderophore transport and/or iron release, this evidences their involvement in THA utilisation. Thus, genetic deletion mutants can be used to infer the use of prospective THAs as siderophores and to identify their transport and iron release mechanisms.

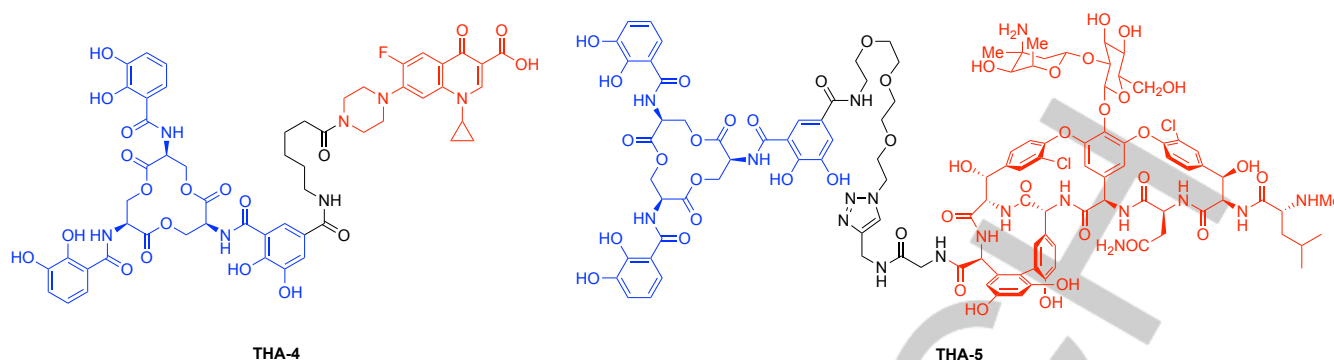


**Figure 14.** Structure of enterobactin conjugates of ciprofloxacin (**THA-4**) and vancomycin (**THA-5**).<sup>[17]</sup> Antibacterial parts in red and siderophore parts in blue.

In work by Zheng *et al.*, growth recovery experiments were utilised to determine whether enterobactin conjugates of ciprofloxacin (**THA-4**) and vancomycin (**THA-5**) were capable of entering *E. coli* and *P. aeruginosa* via enterobactin transporters (Figure 14).<sup>[17]</sup> Initially, an *E. coli* strain defective in enterobactin synthesis ( $\Delta entA$ ) was grown in the presence of both enterobactin-antibiotic conjugates, under iron-limited and iron-sufficient conditions. Although growth recovery was observed for native and some chemically-modified versions of enterobactin under iron-limitation, relative to 'no addition' controls, this was not the case for the antibiotic conjugates. In fact, the vancomycin conjugate (**THA-5**) produced an inhibitory effect due to iron sequestration. However, in tests with a *P. aeruginosa* strain defective in pyoverdine and pyochelin siderophore biosynthesis ( $\Delta pvd\Delta pch$ ), growth recovery was observed for the ciprofloxacin conjugate (**THA-4**), suggesting its cytoplasmic delivery and indicating that the transport pathways in *P. aeruginosa* can accommodate larger cargos. Similar growth recovery experiments have also been used by Madsen *et al.* to compare the utilisation of a staphyloferrin B epimer to its natural isomer in *S. aureus*.<sup>[28]</sup>

### 5.1 Summary

Growth recovery assays provide a good indication of whether prospective THAs are taken up via siderophore-mediated iron uptake pathways. Moreover, by tailoring the genetic deletion mutants employed, identification of the specific transport pathways utilised is possible. The extent to which growth is recovered can infer THA competitiveness with native siderophores. However, such experiments are unlikely to be possible for highly-active THAs, as growth inhibition due to their mode of action might mask any observable growth recovery.

## 6. Fluorescence Labelling

Conjugates containing suitable fluorophores can be used to monitor uptake, and potentially determine the localisation of THAs on or within bacterial cells (Figure 5E). Although there are some studies into the conjugation of fluorescent labels to siderophores (or use of naturally fluorescent siderophores) to study uptake and image or detect bacterial cells (Figure 15),<sup>[29–32]</sup> these often

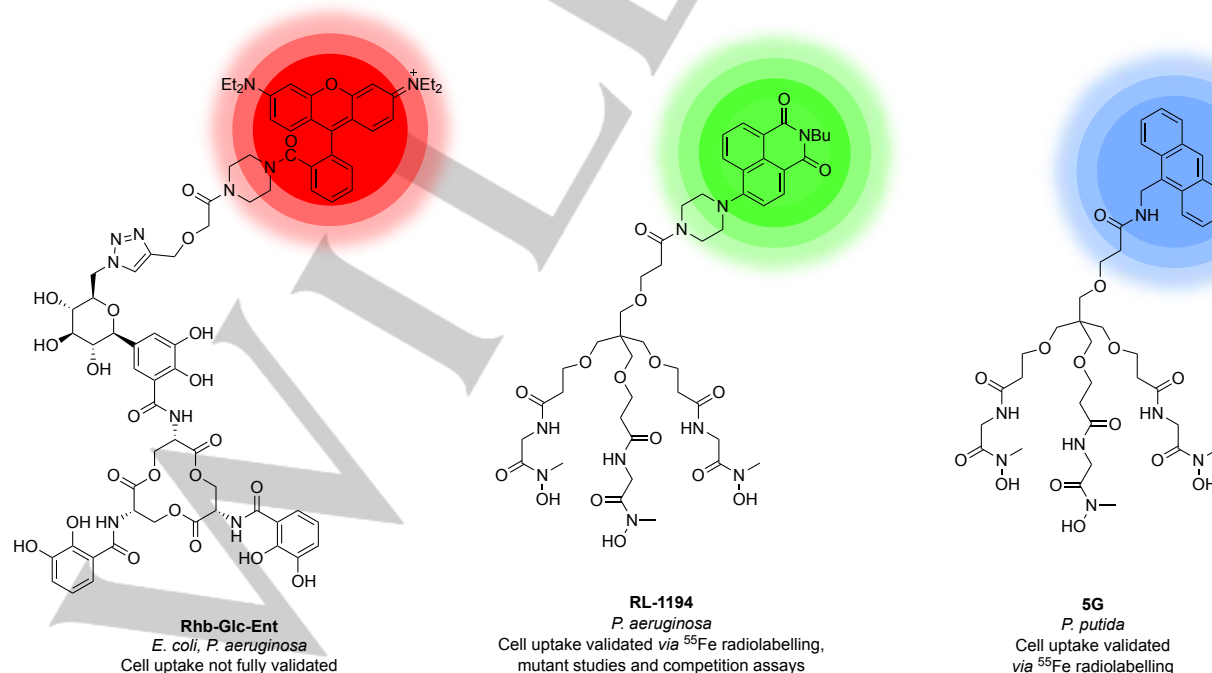


**Figure 15.** Structures of three siderophore-dye conjugates examined for study of bacterial uptake and/or detection of bacterial cells.<sup>[29,30,32]</sup>

## MINIREVIEW

require the use of a complementary method of measuring uptake to confirm passage through the outer membrane, rather than surface or receptor binding with no uptake. In addition, these probes often rely on the direct attachment of a fluorescent dye to a siderophore, generally at a site identical to the conjugation site of the antibacterial unit in THAs. Exchanging a fluorescent dye for an antibacterial bound at the same position is likely to change the overall uptake properties of the conjugate. Attaching both dye and antibiotic to the same siderophore may fall foul of similar problems. Again, these shortcomings may necessitate the use of a complementary method to examine the uptake profiles and validate the results.

A system that has some potential to resolve this issue was reported by Ferreira *et al.*, consisting of a 1,4,7,10-tetraazacyclododecan-1,4,7,10-tetraacetic amide (DOTAM) scaffold bearing catechol groups and a site for antibacterial conjugation (Figure 16).<sup>[33]</sup> The DOTAM scaffold is capable of binding lanthanide ions, such as  $\text{Eu}^{3+}$  or  $\text{Tb}^{3+}$ , which enable luminescent imaging due to their long-lived excited states, although the possibility of sensitised luminescent imaging was not explored at the time. A previous attempt to use a terbium-pyochelin complex to study uptake displayed mixed results.<sup>[34]</sup>

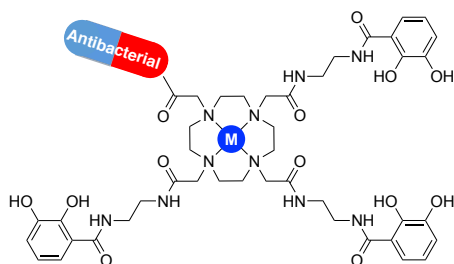


**Figure 16.** General structure of DOTAM scaffolds reported by Ferreira *et al.*<sup>[33]</sup>

A series of artificial hydroxypyridone-based siderophore mimics bound to fluorophores have been examined as antimicrobial agents, primarily in macrophage models (e.g. MRH7, Figure 17).<sup>[35]</sup> While the conjugates do not appear to be internalised in bacteria, the fluorophores seem to play an important part in activity, allowing the conjugates to permeate the cell membranes of macrophages to allow intracellular bacterial targeting. The fluorescence of the conjugates can also be used to track uptake and localisation in macrophages *via* confocal microscopy (Figure 18).<sup>[35,36]</sup> Although not strictly THAs (in that they lack a traditional antimicrobial), they have shown activity against a range of bacteria, including *Mycobacterium avium* and *S. aureus*.<sup>[35]</sup> The conjugates have comparable iron-binding strength to bacterial siderophores, in particular mycobactin, and are suggested to act *via* chelation of  $\text{Fe}^{3+}$ , thereby restricting the supply available to the bacteria.

An alternative approach is the use of fluorescent dyes capable of permeating bacterial cells and detecting siderophore uptake. Calcein (Figure 19) has been shown to bind  $\text{Fe}^{3+}$ , resulting in fluorescence quenching.<sup>[37]</sup> Its acetoxymethyl derivative, calcein-AM, is cell-permeable. On uptake, the acetoxymethyl groups are cleaved, creating an intracellular reserve of calcein.<sup>[11]</sup> Ito *et al.* monitored the uptake of cefiderocol in *P. aeruginosa* over a 5 minute period by observing the relative quenching of calcein on cefiderocol addition.<sup>[11]</sup> This resulted in significant fluorescence

quenching, which implied cefiderocol-mediated iron uptake. Cefiderocol analogues unable to bind iron and the parent antibiotic ceftazidime were used as negative controls, and the native siderophore of *P. aeruginosa*, pyoverdine, served as a positive control. These results indicate that cefiderocol is able to facilitate iron uptake, consistent with acting as a siderophore.<sup>[11]</sup>

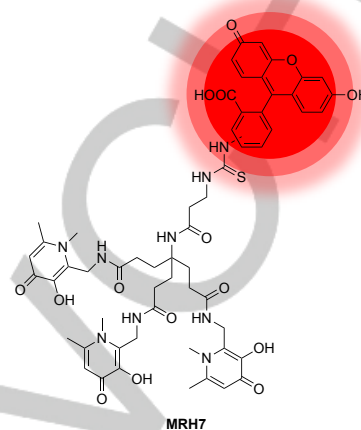


**Figure 17.** Structure of fluorescent chelator MRH7.<sup>[36]</sup>

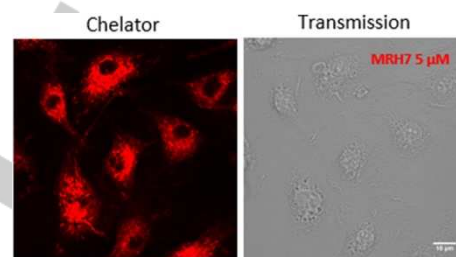


**Figure 18.** Confocal microscopy images of the intracellular distribution of MRH7 in bone marrow-derived macrophages. Reprinted from T. Moniz *et al.*, *J. Inorg. Biochem.*, 2017, 175, 138-147 with permission from Elsevier.<sup>[36]</sup>

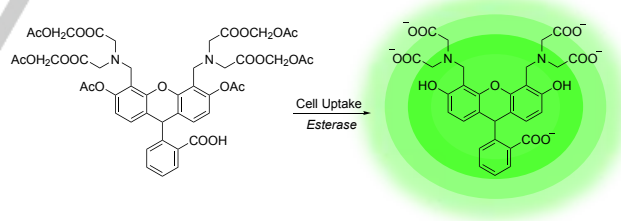


**Figure 19.** Structure of calcein-AM and its intracellular transformation to the fluorescent dye calcein.

### 6.1 Summary

Fluorescent dyes are a less commonly used resource for studying THA uptake. Unless the antibacterial desired for siderophore conjugation is fluorescent itself, the uptake of fluorescently-labelled siderophore conjugates can only be used to loosely infer uptake of the corresponding antibacterial conjugate. Moreover, the incorporation of fluorescent dyes in dual dye-siderophore complexes presents a synthetic challenge and the use of luminescent lanthanide complexes has seen limited development. Intracellular fluorescent dyes offer a different approach, but may come with concerns about cell permeability, selectivity and cost. That said, dye conjugates do offer an interesting opportunity to study the localisation of THAs in macrophages.

## MINIREVIEW

## 7. Radiolabelling

## 7.1 Iron-55/59 Radiolabelling

Radioisotopes of iron have a long history of use as tracers, stretching back to the early 1930s.<sup>[38]</sup> Two isotopes are primarily used for radiolabelling:  $^{55}\text{Fe}$ , an X-ray emitter ( $t_{1/2} = 2.7$  years), and  $^{59}\text{Fe}$ , a  $\beta^-$  emitter ( $t_{1/2} = 44.5$  days); both are commercially available. The low-energy radiation emitted by  $^{55}\text{Fe}$  means that it can be handled with few precautions, while  $^{59}\text{Fe}$  requires more careful handling.<sup>[39,40]</sup> Their half-lives preclude their use in clinical medicine, but render them convenient for use in a number of fields, including some of the first studies to characterise siderophore uptake pathways.<sup>[41]</sup>

The uptake of a number of early synthetic  $\beta$ -lactam THAs was studied via  $^{55}\text{Fe}$  labelling (Figure 20). Curtis *et al.* observed rapid uptake of a series of catechol-substituted cephalosporins including **THA-6** in *E. coli* H1443, but poor uptake in corresponding  $\Delta\text{tonB}$  and  $\Delta\text{cir}\Delta\text{fiu}$  mutants, indicating uptake via the iron transport system, with both the Cir and Fiu outer membrane receptors involved in recognition and uptake.<sup>[42]</sup>

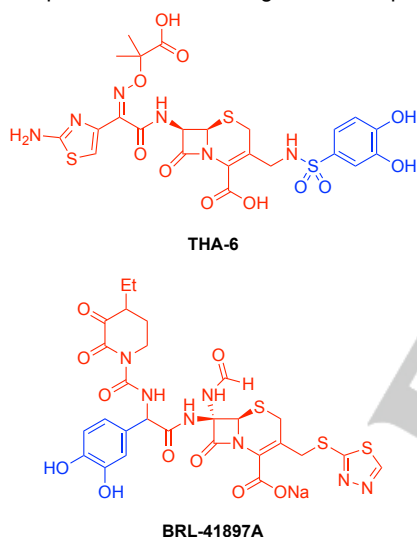


**Figure 20.** Structures of two synthetic  $\beta$ -lactam THAs (**THA-6** and **BRL-41897A**) that have utilised  $^{55}\text{Fe}$  labelling for studying their uptake.<sup>[42,43]</sup> Antibacterial parts in red and siderophore parts in blue.

Nikaido and Rosenberg's study of conjugate E0702, reached a similar conclusion.<sup>[23]</sup> In this case, single mutants of  $\Delta\text{cir}$  and  $\Delta\text{fiu}$  were examined, showing reduced uptake (c. 33% of wild-type), with the  $\Delta\text{cir}\Delta\text{fiu}$  double mutant showing the lowest uptake. A third example studied the uptake of cephalosporin conjugate **BRL-41897A** in *P. aeruginosa*.<sup>[43]</sup> This study concluded uptake occurred via the pyochelin uptake system, with  $^{55}\text{Fe}$ -labelled conjugate uptake greater when the medium was preconditioned by pyochelin, however studies with mutant strains were not carried out. These studies were eventually carried out by Hoegy *et al.* and showed no reduction in antimicrobial activity on removal of the pyochelin outer membrane transporter FptA.<sup>[44]</sup>

Hennard *et al.* used a similar approach to study pyoverdine-fluoroquinolone THAs such as **THA-7** (Figure 21).<sup>[45]</sup> The four examples all demonstrated comparable uptake to the parent

siderophore pyoverdine against *P. aeruginosa* ATCC 15692. Uptake also remained similar in comparison with a mutant strain (IA1) unable to biosynthesise pyoverdine, indicating that the conjugates are responsible for the observed  $^{55}\text{Fe}$  uptake, and that  $^{55}\text{Fe}$  is not being sequestered by native pyoverdine produced by the bacteria. No uptake is observed in a mutant strain lacking the pyoverdine outer membrane receptor FpvA, demonstrating that the conjugates utilise the *P. aeruginosa* pyoverdine uptake pathway.

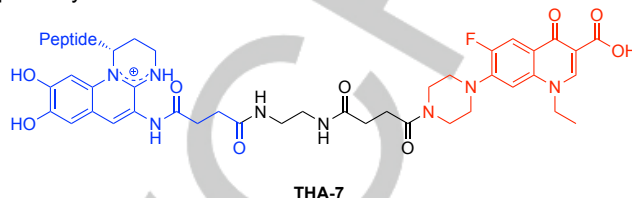


**Figure 21.** Simplified structure of pyoverdine conjugate **THA-7**.<sup>[45]</sup> Antibacterial part in red and siderophore part in blue.

As well as these more direct examples of probing uptake, iron radiolabelling is often used to determine if a given siderophore or siderophore mimic can be taken up by certain species of bacteria, thereby inferring its suitability for use in THAs. An example of this can be seen in the work of Noël *et al.*, who used  $^{55}\text{Fe}$  labelling to confirm that a modified analogue of pyochelin (Figure 22) was transported in an analogous fashion to native pyochelin in *P. aeruginosa*.<sup>[46]</sup>

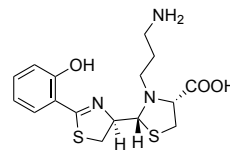


**Figure 22.** Structure of pyochelin analogue reported by Noël *et al.*<sup>[46]</sup>

## 7.2 Gallium-67/68 Radiolabelling

Radioactive gallium isotopes have been used to study siderophores in a similar fashion to  $^{55/59}\text{Fe}$ .  $\text{Ga}^{3+}$  ions have a similar ionic radius to  $\text{Fe}^{3+}$ , and a similar binding affinity to siderophores. In addition, gallium-bound siderophores can be recognised by outer and inner membrane transporters.<sup>[47,48]</sup> Two isotopes of gallium have seen use in radiochemical and medicinal applications:  $^{67}\text{Ga}$ , a gamma emitter ( $t_{1/2} = 3.3$  days), and  $^{68}\text{Ga}$ , a positron emitter ( $t_{1/2} = 68$  min).  $^{67}\text{Ga}$  requires cyclotron synthesis,<sup>[49]</sup> with implications for frequency of supply and availability, but is commercially available, while  $^{68}\text{Ga}$  can be synthesised from  $^{68}\text{Ge}$  ( $t_{1/2} = 271$  days) using a commercial  $^{68}\text{Ge}/^{68}\text{Ga}$  generator.<sup>[49]</sup>

Emery and Hoffer were the first to employ radioactive Ga to study siderophore uptake, with  $^{67}\text{Ga}$ -labelled ferrichrome displaying an analogous uptake profile to  $^{59}\text{Fe}$ -radiolabelled ferrichrome in the fungus *Ustilago sphaerogena*.<sup>[50]</sup> More recently, Petrik *et al.* have carried out extensive studies on the *in vitro* and *in vivo* uptake of a range of  $^{68}\text{Ga}$ -siderophore conjugates by pathogens like *A. fumigatus* and *P. aeruginosa*, with a view to developing techniques for the detection and imaging of human infections (Figure 23).<sup>[51,52]</sup>

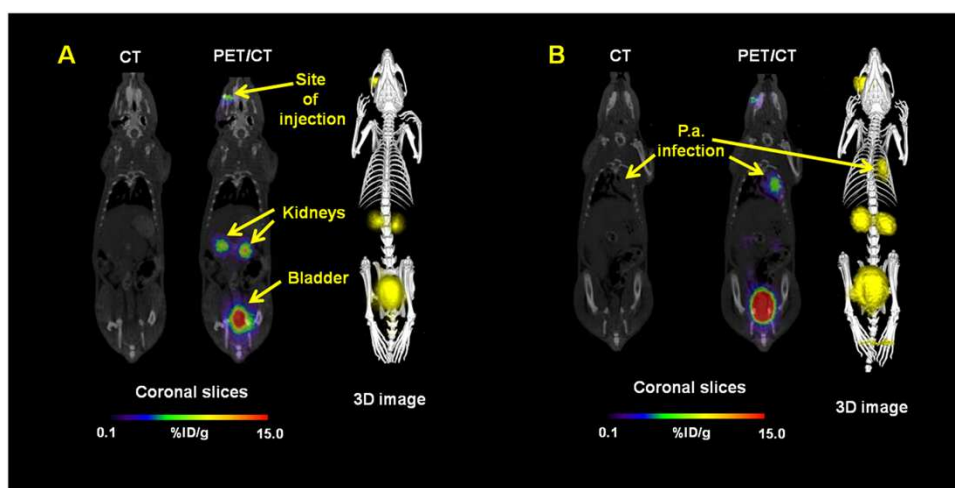


**Figure 23.** Static PET/CT imaging of  $^{68}\text{Ga}$ -pyoverdine-PAO1 in non-infected (A) and intratracheally infected (B) Lewis rats 45 minutes after infection. Reproduced from Petrik *et al.*, *Sci. Rep.*, 2018, 8, 15698 under a Creative Commons licence <http://creativecommons.org/licenses/by/4.0/>.<sup>[52]</sup>

However, there has been little use of radioactive Ga labelling for study of THA uptake. Pandey *et al.* synthesised THAs of both DFO (**THA-8**) and linear desferrichrome (**THA-9**) (Figure 24) with ciprofloxacin as the antibacterial component, observing high activity *versus S. aureus*, *E. coli*, and *P. aeruginosa*.<sup>[48]</sup> Uptake studies with  $^{67}\text{Ga}$  were carried out in *E. coli*, and measured over a two-hour period.  $^{67}\text{Ga}$ -citrate was used as a control; while citrate can be utilised as a siderophore, it displays minimal uptake (<10%), with higher-efficiency siderophores expected to outperform it. Indeed, this is the case for all of the conjugates tested (Figure 25). As might be expected, uptake is increased in iron-limited conditions. The uptake trends do not directly correlate with antibacterial activity; **THA-8** shows higher uptake than **THA-9** (1.5-2x), but slightly reduced antibacterial activity. Sanderson *et al.* carried out similar studies on a salmochelin-inspired conjugate (**THA-10**, Figure 26), which proved poorly active against two *E. coli* strains.<sup>[53]</sup>  $^{67}\text{Ga}$  uptake studies revealed that this was in part due to poor cellular uptake, with **THA-10** taken up at comparable levels to  $^{67}\text{Ga}$ -citrate.

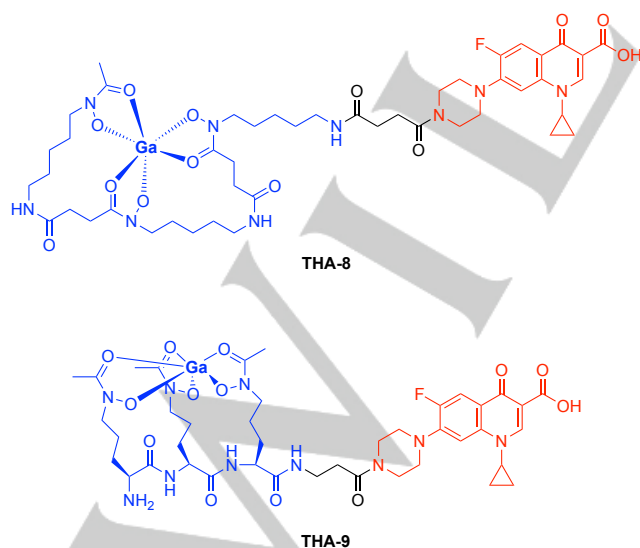


**Figure 24.** Structures of Ga complexes of **THA-8** and **THA-9** reported by Pandey *et al.*<sup>[48]</sup> Antibacterial parts in red and siderophore parts in blue.

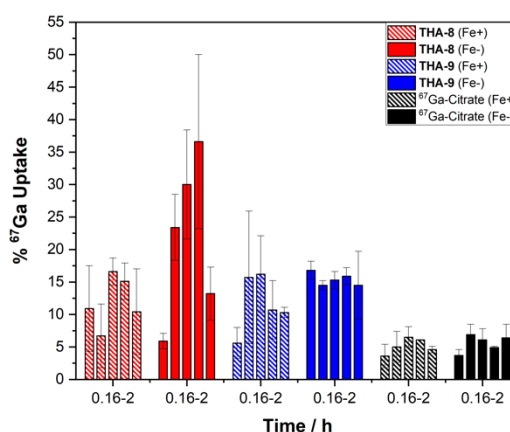


**Figure 25.** Results of **THA-8** and **THA-9** radiochemical uptake studies in *E. coli* for iron-sufficient (striped bars) and iron-limited conditions (solid bars).  $^{67}\text{Ga}$  citrate is included for comparison.<sup>[48]</sup> Measurements were taken at 0.16 h, 0.33 h, 0.50 h, 1 h and 2 h timepoints.

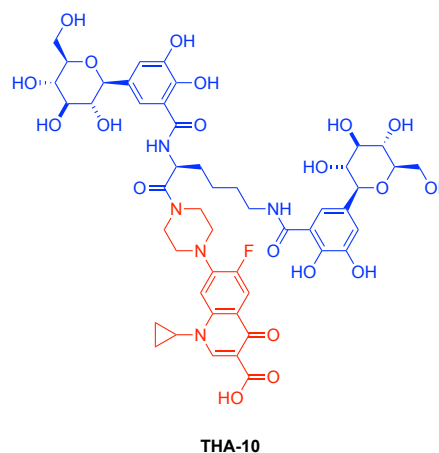


**Figure 26.** Structure of a salmochelin-inspired conjugate (**THA-10**).<sup>[53]</sup> Antibacterial part in red and siderophore part in blue.

## MINIREVIEW

## 7.3 Tritium/Carbon-14 Radiolabelling

In addition to complexation with radioactive metals, labelling of THAs with radioisotopes such as tritium ( $^3\text{H}$ ,  $t_{1/2} = 12.3$  years) or carbon-14 ( $^{14}\text{C}$ ,  $t_{1/2} = 5730$  years) can be carried out. Both radioisotopes are only weak  $\beta^-$  emitters, enabling their use with relatively few precautions.<sup>[54]</sup> In terms of synthesis,  $^3\text{H}$  can be installed *via* hydrogen/tritium exchange, whereas  $^{14}\text{C}$  incorporation often requires longer, more involved synthetic routes, or supplementation of growth media with  $^{14}\text{C}$ -labelled feedstocks.<sup>[54,55]</sup> However,  $^3\text{H}$  is often considered more susceptible to metabolism and removal.<sup>[55]</sup>

Both techniques have been widely used in the study of siderophore uptake, often alongside iron or gallium radiolabelling, gaining further insight into the uptake and utilisation of siderophores.<sup>[56,57]</sup> For example, the monitoring of both the metal and the organic parts of the siderophore complex allows confirmation that both are taken up together, and the observed metal uptake is not facilitated by other siderophores outcompeting and binding the radiolabelled metal. Hartmann *et al.* used both  $^{55}\text{Fe}$  and  $^3\text{H}$  labelling for the study of the natural sideromycin antibiotic albomycin (Figure 27). They found rapid uptake of  $^{55}\text{Fe}$  ferrichrome, the parent siderophore of albomycin (complete  $^{55}\text{Fe}$  uptake within two minutes). The  $^3\text{H}$ -labelled ferrichrome (complexed to non-radioactive Fe) accumulates over a longer time (50% at 20 minutes), perhaps suggesting siderophore recycling and re-uptake over time. For albomycin,  $^{55}\text{Fe}$  is taken up at a slower rate (c. 50% of ferrichrome), although it eventually reaches similar levels within the cells. However, the  $^3\text{H}$ -labelled component is excluded from the cells entirely over time. Separate radiolabelling of the antibiotic component of albomycin with  $^{35}\text{S}$  showed that 30–40% remained in the cells over 20 minutes, suggesting hydrolysis of the antimicrobial component from the siderophore is crucial for albomycin's activity.

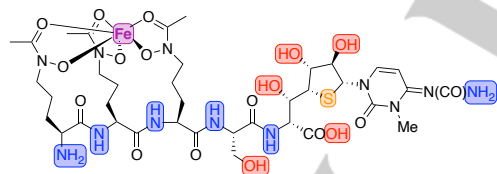


**Figure 27.** Structure of albomycin with potential radiolabelling sites highlighted.<sup>[58]</sup>

In a more recent example, Ito *et al.* used  $^{14}\text{C}$ -labelling to study the uptake of the  $\beta$ -lactam THA cefiderocol in *P. aeruginosa*.<sup>[11]</sup> Uptake experiments were carried out in iron-limited and iron-sufficient MHII. In both cases cefiderocol is taken up rapidly. Overall uptake was 2.5x higher in iron-limited MHII, which correlates well with its increased antibacterial activity under iron-limited conditions. As mentioned above, this can be linked to upregulation of outer membrane siderophore receptors upon iron-limitation, and infers that cefiderocol is taken up *via* siderophore transport pathways. While further evidence was not presented in this paper, later studies revealed reduced antibacterial activity in a genetic deletion mutant of *P. aeruginosa* lacking the PiuA outer membrane receptor, providing further evidence for cefiderocol's proposed use of siderophore uptake pathways.<sup>[59]</sup>

## 7.4 Other Potential Radionuclides

Other radiolabelling strategies have also been used in conjunction with siderophores.  $^{51}\text{Cr}$  has a long record of use in siderophore uptake studies, with its ability to form kinetically inert complexes a particular benefit.<sup>[57,60]</sup>  $^{89}\text{Zr}^{4+}$  and  $^{111}\text{In}^{3+}$ , both hard ions with high coordination numbers, are well-suited to forming complexes with siderophores.<sup>[51,61,62]</sup>  $^{89}\text{Zr}$ , often combined with DFO-derived ligands,<sup>[51,62]</sup> has been examined as a potential radioisotope to study bacterial uptake, with Petrik *et al.* demonstrating analogous *in vitro* / *in vivo* properties to  $^{68}\text{Ga}$ ,<sup>[63]</sup> and Goscinski successfully carrying out uptake studies in *S. aureus* and *P. aeruginosa*.<sup>[64]</sup> However, to the best of our knowledge, none of these three radioisotopes have yet been applied to the study of siderophore THAs.

## 7.5 Summary

While radiolabelling studies require a degree of specialist knowledge and equipment, and the relatively high cost of radionuclides may be prohibitive to their widespread use, radiolabelling of THAs has the potential to offer valuable insights into all stages of their uptake. The introduction of appropriate radionuclides usually has little impact on siderophore recognition and transport, allowing a clear picture of THA uptake to be obtained. The field is also moving more towards theranostic applications, with a number of recent papers making advances in this area.<sup>[33,48,52,65]</sup>

## 8. Summary

A key part of evaluating THAs is the quantification of their uptake into bacteria, and the determination of the specific pathways involved. This information is vital in understanding the scope of use possible for THAs, allowing the improvement of existing designs and development of new strategies. Such studies go hand in hand with research into the identification and characterisation of membrane receptors, as well as other proteins involved in the bacterial internalisation of siderophores, which offer further insight into THA design. A number of techniques for studying uptake are outlined above, from biological studies through to radiolabelling, with each technique offering a unique insight into part of a THA's uptake profile. Many of these techniques are well-precedented, offering researchers a variety of options. However, the sole reliance on particular methods, such as iron-dependent antibacterial activity and competition assays, can lead to misleading results and therefore in these cases, it is recommended supportive studies / appropriate controls are undertaken. Moreover, some methods require experience in specialist techniques (e.g. the synthesis of bacterial genetic deletion mutants or the use of radioactive material) or further development before they could be widely used, for example the use of fluorescent dyes for monitoring uptake is relatively underdeveloped. New complementary techniques, like the multimodal imaging mass spectrometry applied by Perry *et al.* for the mapping of siderophore presence within infected tissues,<sup>[66]</sup> may promise valuable insights into this area in the near future.

## MINIREVIEW

## Acknowledgements

The authors would like to thank Mr. Reyme Herman, from the Department of Biology, University of York, for his advice and comments on the sections regarding the use of bacterial mutant strains. We thank the UK Engineering and Physical Research Council (EPSRC) for financial support: grant EP/T007338/1 (A.-K. Duhme-Klair) and studentship EP/N509802/1 (C. M. Black), and the University of York for a Teaching Studentship (J. W. Southwell). BioRender.com was employed for the design of the frontispiece, and Figures 3 and 5. Figures 9 and 18 are reprinted with permission from ACS and Elsevier respectively; further enquiries regarding permissions for these figures should be directed to them.

**Keywords:** antibiotics • iron uptake • siderophores • Trojan Horse antibacterials

- [1] R. C. Hider, X. Kong, *Nat. Prod. Rep.* **2010**, 27, 637–657.
- [2] M. Miethke, M. A. Marahiel, *Microbiol. Mol. Biol. Rev.* **2007**, 71, 413–451.
- [3] H. Lin, M. A. Fischbach, D. R. Liu, C. T. Walsh, *J. Am. Chem. Soc.* **2005**, 127, 11075–11084.
- [4] K. Hantke, *Mol. Gen. Genet.* **1981**, 182, 288–292.
- [5] L. Zimmermann, K. Hantke, V. Braun, *J. Bacteriol.* **1984**, 159, 271–277.
- [6] V. Braun, A. Pramanik, T. Gwinner, M. Köberle, E. Bohn, *BioMetals* **2009**, 22, 3–13.
- [7] *Antibacterial Agents in Clinical Development*, Geneva, **2017**.
- [8] M. S. Butler, M. A. Blaskovich, M. A. Cooper, *J. Antibiot. (Tokyo)* **2013**, 66, 571–591.
- [9] M. G. P. Page, *Clin. Infect. Dis.* **2019**, 69, S529–S537.
- [10] K. N. Raymond, E. A. Dertz, S. S. Kim, *Proc. Natl. Acad. Sci.* **2003**, 100, 3584–3588.
- [11] A. Ito, T. Nishikawa, S. Matsumoto, H. Yoshizawa, T. Sato, R. Nakamura, M. Tsuji, Y. Yamano, *Antimicrob. Agents Chemother.* **2016**, 60, 7396–7401.
- [12] N. Kohira, J. West, A. Ito, T. Ito-Horiyama, R. Nakamura, T. Sato, S. Rittenhouse, M. Tsuji, Y. Yamano, *Antimicrob. Agents Chemother.* **2016**, 60, 729–734.
- [13] T. M. A. Santos, M. G. Lammers, M. Zhou, I. L. Sparks, M. Rajendran, D. Fang, C. L. Y. De Jesus, G. F. R. Carneiro, Q. Cui, D. B. Weibel, *ACS Chem. Biol.* **2018**, 13, 235–246.
- [14] Q. Laurent, L. K. Batchelor, P. J. Dyson, *Organometallics* **2018**, 37, 915–923.
- [15] T. A. Wencewicz, T. E. Long, U. Möllmann, M. J. Miller, *Bioconjug. Chem.* **2013**, 24, 473–486.
- [16] T. Zheng, E. M. Nolan, *J. Am. Chem. Soc.* **2014**, 136, 9677–9691.
- [17] T. Zheng, J. L. Bullock, E. M. Nolan, *J. Am. Chem. Soc.* **2012**, 134, 18388–18400.
- [18] J. A. Goldberg, H. Nguyen, V. Kumar, E. J. Spencer, D. Hoyer, E. K. Marshall, A. Cmolik, M. O'Shea, S. H. Marshall, A. M. Hujer, K. M. Hujer, S. D. Rudin, T. N. Domitrovic, C. R. Bethel, K. M. Papp-Wallace, L. K. Logan, F. Perez, M. R. Jacobs, D. van Duin, B. M. Kreiswirth, R. A. Bonomo, M. S. Plummer, F. van den Akker, *J. Med. Chem.* **2020**, 63, 5990–6002.
- [19] C. Ji, P. A. Miller, M. J. Miller, *J. Am. Chem. Soc.* **2012**, 134, 9898–9901.
- [20] C. J. McPherson, L. M. Aschenbrenner, B. M. Lacey, K. C. Fahnoe, M. M. Lemmon, S. M. Finegan, B. Tadakamalla, J. P. O'Donnell, J. P. Mueller, A. P. Tomaras, *Antimicrob. Agents Chemother.* **2012**, 56, 6334–6342.
- [21] T. A. Wencewicz, M. J. Miller, *J. Med. Chem.* **2013**, 56, 4044–4052.
- [22] U. Möllmann, L. Heinisch, A. Bauernfeind, T. Köhler, D. Ankel-Fuchs, *BioMetals* **2009**, 22, 615–624.
- [23] H. Nikaido, E. Y. Rosenberg, *J. Bacteriol.* **1990**, 172, 1361–1367.
- [24] K. Hantke, *FEMS Microbiol. Lett.* **1990**, 67, 5–8.
- [25] L. Moynié, A. Luscher, D. Rolo, D. Pletzer, A. Tortajada, H. Weingart, Y. Braun, M. G. P. Page, J. H. Naismith, T. Köhler, *Antimicrob. Agents Chemother.* **2017**, 61, e02531-16.
- [26] C. van Delden, M. G. P. Page, T. Köhler, *Antimicrob. Agents Chemother.* **2013**, 57, 2095–2102.
- [27] A. P. Tomaras, J. L. Crandon, C. J. McPherson, M. A. Banevicius, S. M. Finegan, R. L. Irvine, M. F. Brown, J. P. O'Donnell, D. P. Nicolau, *Antimicrob. Agents Chemother.* **2013**, 57, 4197–4207.
- [28] J. L. H. Madsen, T. C. Johnstone, E. M. Nolan, *J. Am. Chem. Soc.* **2015**, 137, 9117–9127.
- [29] H. Weizman, O. Ardon, B. Mester, J. Libman, O. Dwir, Y. Hadar, Y. Chen, A. Shanzer, *J. Am. Chem. Soc.* **1996**, 118, 12368–12375.
- [30] M. Hannauer, Y. Barda, G. L. A. Mislin, A. Shanzer, I. J. Schalk, *J. Bacteriol.* **2010**, 192, 1212–1220.
- [31] T. Zheng, E. M. Nolan, *Metallomics* **2012**, 4, 866–880.
- [32] A. A. Lee, Y.-C. S. Chen, E. Ekalestari, S.-Y. Ho, N.-S. Hsu, T.-F. Kuo, T.-S. A. Wang, *Angew. Chemie Int. Ed.* **2016**, 55, 12338–12342.
- [33] K. Ferreira, H.-Y. Hu, V. Fetz, H. Prochnow, B. Rais, P. P. Müller, M. Brönstrup, *Angew. Chemie Int. Ed.* **2017**, 56, 8272–8276.
- [34] B. Yang, F. Hoegy, G. L. A. Mislin, P. J. Mesini, I. J. Schalk, *J. Inorg. Biochem.* **2011**, 105, 1293–1298.
- [35] M. Rangel, T. Moniz, A. M. N. Silva, A. Leite, *Pharmaceuticals* **2018**, 11, 110, and references therein.
- [36] T. Moniz, A. Leite, T. Silva, P. Gameiro, M. S. Gomes, B. de Castro, M. Rangel, *J. Inorg. Biochem.* **2017**, 175, 138–147.
- [37] F. Thomas, G. Serratrice, C. Béguin, E. S. Aman, J. L. Pierre, M. Fontecave, J. P. Laulhère, *J. Biol. Chem.* **1999**, 274, 13375–13383.
- [38] J. G. Hamilton, *J. Appl. Phys.* **1941**, 12, 541–572, and references therein.
- [39] PerkinElmer, "Iron-55 Handling Precautions," can be found under [https://www.perkinelmer.com/lab-solutions/resources/docs/TCH\\_Iron55.pdf](https://www.perkinelmer.com/lab-solutions/resources/docs/TCH_Iron55.pdf), **2010**.
- [40] PerkinElmer, "Iron-59 Handling Precautions," can be found under [https://www.perkinelmer.com/lab-solutions/resources/docs/TCH\\_Iron59.pdf](https://www.perkinelmer.com/lab-solutions/resources/docs/TCH_Iron59.pdf), **2010**.
- [41] C. E. Lankford, B. R. Byers, *CRC Crit. Rev. Microbiol.* **1973**, 2, 273–331, and references therein.
- [42] N. A. Curtis, R. L. Eisenstadt, S. J. East, R. J. Cornford, L. A. Walker, A. J. White, *Antimicrob. Agents Chemother.* **1988**, 32, 1879–1886.
- [43] K. Gensberg, E. J. Doyle, D. J. Perry, A. W. Smith, *J. Antimicrob. Chemother.* **1994**, 34, 697–705.
- [44] F. Hoegy, M. N. Gwynn, I. J. Schalk, *Amino Acids* **2010**, 38, 1627–1629.
- [45] C. Hennard, Q. C. Truong, J. F. Desnottes, J. M. Paris, N. J. Moreau, M. A. Abdallah, *J. Med. Chem.* **2001**, 44, 2139–2151.

## MINIREVIEW

- [46] S. Noël, V. Gasser, B. Pesset, F. Hoegy, D. Rognan, I. J. Schalk, G. L. A. Mislin, *Org. Biomol. Chem.* **2011**, *9*, 8288–8300.
- [47] T. E. Clarke, V. Braun, G. Winkelmann, L. W. Tari, H. J. Vogel, *J. Biol. Chem.* **2002**, *277*, 13966–13972.
- [48] A. Pandey, C. Savino, S. H. Ahn, Z. Yang, S. G. Van Lanen, E. Boros, *J. Med. Chem.* **2019**, *62*, 9947–9960.
- [49] M. A. Synowiecki, L. R. Perk, J. F. W. Nijssen, *EJNMMI Radiopharm. Chem.* **2018**, *3*, 3.
- [50] T. Emery, P. Hoffer, *J. Nucl. Med.* **1980**, *21*, 935–939.
- [51] M. Petrik, C. Zhai, H. Haas, C. Decristoforo, *Clin. Transl. Imaging* **2017**, *5*, 15–27, and references therein.
- [52] M. Petrik, E. Umlaufova, V. Raclavsky, A. Palyzova, V. Havlicek, H. Haas, Z. Novy, D. Dolezal, M. Hajduch, C. Decristoforo, *Sci. Rep.* **2018**, *8*, 15698.
- [53] T. J. Sanderson, C. M. Black, J. W. Southwell, E. J. Wilde, A. Pandey, R. Herman, G. H. Thomas, E. Boros, A.-K. Duhme-Klair, A. Routledge, *ACS Infect. Dis.* **2020**, *6*, 2532–2541.
- [54] J. Atzrodt, V. Derdau, W. J. Kerr, M. Reid, *Angew. Chemie Int. Ed.* **2018**, *57*, 1758–1784.
- [55] J. A. Krauser, *J. Labelled Comp. Radiopharm.* **2013**, *56*, 441–446.
- [56] J. Leong, J. B. Neillands, *J. Bacteriol.* **1976**, *126*, 823–830.
- [57] A. Stintzi, C. Barnes, J. Xu, K. N. Raymond, *Proc. Natl. Acad. Sci.* **2000**, *97*, 10691–10696.
- [58] A. Hartmann, H.-P. Fiedler, V. Braun, *Eur. J. Biochem.* **1979**, *99*, 517–524.
- [59] A. Ito, T. Sato, M. Ota, M. Takemura, T. Nishikawa, S. Toba, N. Kohira, S. Miyagawa, N. Ishibashi, S. Matsumoto, R. Nakamura, M. Tsuji, Y. Yamano, *Antimicrob. Agents Chemother.* **2018**, *62*, e01454-17.
- [60] D. J. Ecker, T. Emery, *J. Bacteriol.* **1983**, *155*, 616–622.
- [61] S. M. Moerlein, M. J. Welch, K. N. Raymond, F. L. Weill, *J. Nucl. Med.* **1981**, *22*, 710–719.
- [62] E. Boros, A. B. Packard, *Chem. Rev.* **2019**, *119*, 870–901.
- [63] M. Petrik, C. Zhai, Z. Novy, L. Urbanek, H. Haas, C. Decristoforo, *Mol. Imaging Biol.* **2016**, *18*, 344–352.
- [64] N. C. M. Goscinski, Investigation of  $^{89}\text{Zr}$ -Siderophores as Molecular Imaging Agents for Positron Emission Tomography Imaging of Bacterial Infections, Washington University, **2015**.
- [65] M. Petrik, J. Pfister, M. Misslinger, C. Decristoforo, H. Haas, *J. Fungi* **2020**, *6*, 73, and references therein.
- [66] W. J. Perry, J. M. Spraggins, J. R. Sheldon, C. M. Grunenwald, D. E. Heinrichs, J. E. Cassat, E. P. Skaar, R. M. Caprioli, *Proc. Natl. Acad. Sci.* **2019**, *116*, 21980–21982.

## MINIREVIEW

## Entry for the Table of Contents

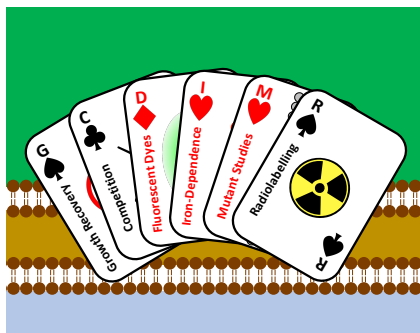


**Table of Contents Text:** Siderophore-based Trojan Horse antibacterials offer an opportunity to exploit specific iron uptake pathways for drug delivery. Understanding the mechanisms by which these compounds are taken up, if at all, is vital to their continued development. We present a selection of complementary methods that have been employed to examine the uptake of Trojan Horse antibacterials.

**Institute:** University of York

**Twitter username:** @DuhmeKlairYork